JOC Article

Biogenesis of Sesquiterpene Lactones Pseudoguaianolides from Germacranolides: Theoretical Study on the Reaction Mechanism of Terminal Biogenesis of 8-Epiconfertin

José Enrique Barquera-Lozada and Gabriel Cuevas*

Instituto de Química, Universidad Nacional Autónoma de México, Apdo. Postal 70213, 04510, Coyoacán, Circuito Exterior, México D.F. México

gecgb@servidor.unam.mx

Received November 2, 2008

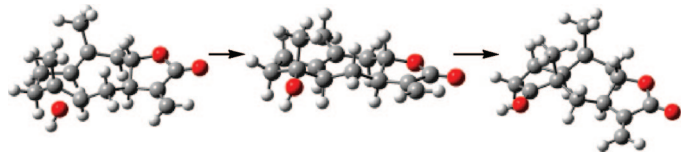

The fundamental study of the biogenetic origin of natural products has always been limited from the experimental point of view because proposed reaction mechanisms have only been supported on the molecular structures of reagents and the reaction products. In a seminal contribution, Ortega and Maldonado (Ortega, A.; Maldonado, E. *Heterocycles*, **1989**, *29*, 635−638.) described an experiment relevant for the development of the biogenetic theory of sesquiterpene lactones. They were able to obtain the one-pot transformation of a pseudoguaianolide sesquiterpenic lactone from a germacranolide using bentonitic earth as the catalyst. This transformation involved two steps in the biogenesis of these compounds (germacranolide → guaianolide → pseudoguaianolide) and is significant because when Brönsted or Lewis acids are used, it is only possible to isolate the product of the next step of the biogenesis. The results presented here support the biogenetic theories by Hendrickson and Fischer and question the concerted nature of the Herz proposal. Some questions about the mechanisms still remain unanswered; mainly because it was only possible to isolate a few stable byproducts. Using the third generation functional mPWB95 developed by Truhlar, it was possible to study the mechanisms associated with the biogenesis of pseudoguaiananolides. Its application can explain the origin of all the byproducts obtained in the original experiment and establish the validity of the original biogenetic hypothesis. The performance of the above-mentioned functional was compared to B3LYP, B97−2, and B1B95 functionals and the MP2 method, finding that mPWB95 competes successfully with all the latter in both, the determination of the magnitude of the activation energies and the ability to map the potential energy surface. Therefore, the mPWB95 method can be considered good to deal with this type of study.

Introduction

Natural products have a wide variety of chemical structures that characterize the various species inhabiting the world. Curiously, such a diverse variety of chemical compounds is produced using only a very limited number of biosynthetic routes.[1] This may be, yet another example of the efficiency that commonly prevails in Nature.[2] For example, mevalonic acid is the origin of all terpenes and terpenoids in superior organisms while 1-deoxy-D-xylulose-5-phosphate is used by lesser organisms.[3,4] On the other hand, all the sesquiterpenes used by superior organisms have their origin in either farnesol (specifically the farnesyl pyrophosphate FPP, **1-a** Scheme 1) or nerolidyl pyrophosphate.[5−7] Natural products, particularly secondary metabolites, condition the adaptability of species and thus, their

(1) Richards, J. H.; Hendrickson, J. B. *The biosinthesis of steroids, terpenes and acetogenins*; Benjamín: New York, 1964.
(2) Lehninger, A. L. *Biochemistry*; Worth Publisher: New York, 1970; p 483.
(3) Kuzuyama, T.; Seto, H. *Nat. Prod. Rep.* **2003**, *20*, 171–183.
(4) Rohmer, M.; Seemann, M.; Horbach, S.; Bringer-Meyer, S.; Sahm, H. *J. Am. Chem. Soc.* **1996**, *118*, 2564–2566.
(5) Cane, D. E. *Pure Appl. Chem.* **1989**, *61*, 493–496.
(6) Fischer, N. H.; Olivier, E. J.; Fischer, H. D. The Biogenesis and Chemistry of sesquiterpene Lactones. In *Progress in the Chemistry of Organic Natural Products*; Herz, W., Grisebach, H., Kirby, G. W., Eds.; Springer-Verlag: Wien, 1979; p 47.
(7) Romo de Vivar, A. *Rev. Latinoam. Quim.* **1977**, *8*, 63–73; *Chem Abst.* **1977**, *87*, 18934.

10.1021/jo802445n CCC: $40.75
Published on Web 12/04/2008

SCHEME 1. Structure of the Configurational Isomers Produced by the First Biogenetic Stage, the Closure of FPP

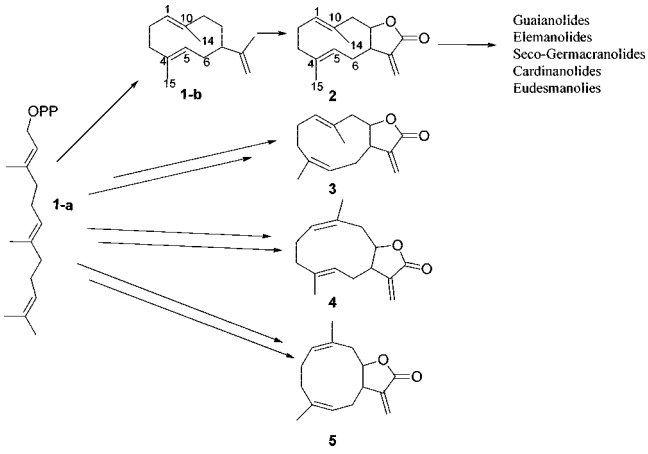

survival and evolution. Nowadays, several fundamental aspects of the mevalonate and nonmevalonate pathways such as the enzymes that catalyze their transformation and the genes that codify for them are well-known.[8] The terminal biogenesis of the different natural products responsible for the great structural diversity of compounds has been rarely studied and there are still many unanswered questions on the mechanisms responsible for generating such a variety of molecules.[9−18] Chemical simulation of biogenetic processes is based on the fact that the reactions that take place *in vivo* follow the same general principles of *in vitro* transformations.[19] Using this technique, one can demonstrate that, in many cases, a complex enzymatic system is not really necessary to maintain control of several aspects such as in *situ*, *stereo* and *regio*-selectivity. Enzymes seem fundamental for the selection of the starting conformer and explain the high chemical yields of these transformations; however, one or two steps of the biogenetic process can be simulated *in vitro.*[20–22]

CHART 1

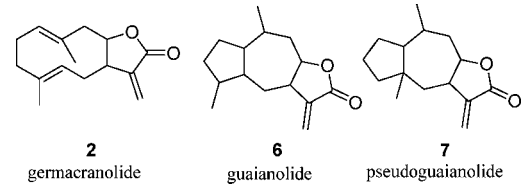

Sesquiterpene synthetases generate cyclic compounds from FPP (**1-a**, Scheme 1) and control their subsequent transformation into more than 300 different sesquiterpenes. These enzymes and their action have been widely studied.[23] T*rans,trans*-germacradiene (**1-b**, Scheme 1) is obtained from the direct cyclization process of *trans,trans*-FPP (or *E,E*-FPP), an intermediate that is transformed by enzymatic oxidative modification to yield the corresponding lactones. Two possible biogenetic routes have been suggested for the formation of the lactone ring of these sesquiterpenoids.[13,15,16] On the first biogenetic stage, there are four possible configurational isomers: the germacrolides of configuration C1-E, C4-E (**2**, Scheme 1), the heliangolides (**3**) (C1-E, C4-Z), the melampolides (**4**) (C1-Z, C4-E) and the Z,Z germacranolides (**5**). This was demonstrated by the isolation of compounds with four possible configurations.[24]

According to Fischer,[16,24] on the second biogenetic stage, five different types of skeletons are produced from the germacranolide. These are the guaianolides, eudesmanolides, elemanolides, seco-germacranolides, and cadinanolides (Scheme 1).

In this paper, we approach the study of the ring closure suffered by the germacranolides (**2**) to produce guaianolides (**6**, Chart 1). This is the second stage in the biogenesis that evolves to the third stage when the methyl at position C4 migrates to position C5 originating pseudoguaianolides (**7**, Chart 1). This study evaluates the proposed biogenetic theories for the formation of guaianolides and pseudoguaianolides[9,25] using computational methods. We also study the formation of such structural diverse compounds that can exert a wide variety of biological functions in nature (antifeedant, cytotoxic, insecticide, etc.) and that serve as useful chemical markers for the classification of plants and the establishment of their taxonomic relations and level of evolution.[26]

The recent seminal contributions of Gao[27,28] and Truhlar,[23,29] Tantillo,[30–33] Corey,[34] Jorgensen,[35] and Hess[36–39] where the biogenesis of natural products is approached using computational methods show the potential application of this methodology due to its usefulness in establishing the reaction mechanisms by which these transformations occur. Computational methods are a good alternative to the lack of experimental data frequently experienced. Moreover, the new functionals developed by Truhlar allow substantial improvements in the description of reactive systems as it will be shown in this paper. The methodology can also be used to evaluate the participation of the enzymatic systems that control these transformations.

To the best of our knowledge, the first application of computational methods oriented to the study of the transforma-

(8) Cane, D. E. *Chem. Rev.* **1990**, *90*, 1089–1103.
(9) Hendrickson, J. B. *Tetrahedron* **1959**, *7*, 82–89.
(10) Barton, D. H. R.; Bockmann, O. C.; de Mayo, P. *J. Chem. Soc.* **1960**, 2263–2271.
(11) (a) Ruzicka, L. *Experientia* **1953**, *9*, 357–367. (b) Ruzicka, L. *Pure Appl. Chem.* **1963**, *6*, 493–523.
(12) Parker, W.; Roberts, J. S.; Ramaje, R. *Quart. Rev.* **1967**, *21*, 331–363.
(13) (a) Herz, W. Sesquitepene Lactones Biogenesis. In *Pharmacognosy and Phytochemistry*; Wagner, H., Horhammer, L., Eds.; Springer-Verlag: West Berlin and Heildelberg, 1971; p 64. (b) Herz, W. *Isr. J. Chem.* **1977**, *16*, 32–44.
(14) Hanson, J. R. *Terpenoid Biosyntheis in Comprehensive Organic Chemistry*; Barton, D. H. R., Ed.; Academic Press, New York 1979; Chapter 29.
(15) Geissman, T. A. *Rec. Adv. Phytochem.* **1973**, *6*, 65–95.
(16) Fischer, N. H.; Oliver, E. J.; Fischer, H. D. *Prog. Chem. Org. Nat. Prod.* **1979**, *38*, 77–390.
(17) (a) Cane, D. E. *Isoprenoids Including Carotenoids and Steroids*; Cane, D. E., Ed.; Comprehensive Natural Products Chemistry, Vol. 2; Elsevier: Oxford, 1999; p 155. (b) Felicetti, B.; Cane, D. E. *J. Am. Chem. Soc.* **2004**, *126*, 7212.
(18) (a) Goodwin, T. W., Ed. *Natural substances formed biologically from mevalonic acid*; Biochemical Symposia No. 29; Academic Press: New York, 1970. (b) MacMillan, J. *Recent Adv. Phytochem.* **1974**, *7*, 1–19. (c) Delgado, G. Investigación sobre la Química de productos naturales en el Instituto de Química de la UNAM. Estudios iniciales y química de eremofilanos, bisabolanos y sesquiterpenos relacionados. In *Química de la flora mexicana*; Romo de Vivar, A., Ed.; Instituto de Química: Mexico, 2006. (d) Christianson, D. W. *Chem. Rev.* **2006**, *106*, 3412–3442. (e) Dewick, P. M. *Nat. Prod. Rep.* **1999**, *16*, 97–130. (f) Dewick, P. M. *Nat. Prod. Rep.* **2002**, *19*, 181–272. (g) Steel, C. L.; Crock, J.; Bohlman, J.; Croteau, R. *J. Biol. Chem.* **1998**, *273*, 2078. (h) Starcks, C. M.; Back, K.; Chapell, J.; Noel, J. P. *Science* **1997**, *277*, 1815–1820.
(19) (a) Herrera, A. L. *Science* **1942**, *96*, 2479–14. (b) Negrón-Mendoza, A. *J. Biol. Phys.* **1994**, *20*, 11–15.
(20) Coates, R. M. *Prog. Chem. Org. Nat. Prod.* **1976**, *33*, 73–230.
(21) Goldsmith, D. *Prog. Chem. Org. Nat. Prod.* **1971**, *29*, 363–394.
(22) Money, T. *Prog. Org. Chem.* **1973**, *8*, 29–77.
(23) (a) Allermann, R. K.; Young, N. J.; Ma, S.; Truhlar, D. G.; Gao, J. *J. Am. Chem. Soc.* **2007**, *129*, 13008–13013. (b) Chapell, J. *Annu. Rev. Plant Physiol. Plant Mol. Biol.* **1995**, *46*, 521–547. (c) McCaskill, D.; Croteau, R. *Planta* **1995**, *197*, 49–56. (d) vanKlink, J.; Becker, H.; Anderson, S.; Boland, W. *Org. Biomol. Chem.* **2003**, *1*, 1503–1508.
(24) Fischer, N. H. *Rev. Latinoam. Quím.* **1978**, *9*, 41–46.
(25) Fischer, H. H.; Wu-Shih, Y. F.; Chiari, G.; Fronczek, F. R.; Watkins, S. F. *J. Nat. Prod.* **1981**, *44*, 104–110.
(26) Zdero, C.; Bohlmann, F. *Phytochemistry* **1989**, *28*, 1653–1660.

CHART 2

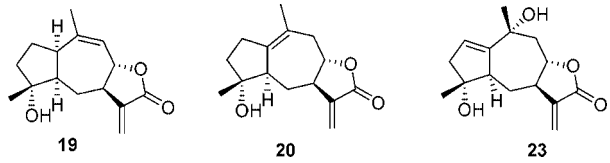

tion of sesquiterpenic lactones was reported by Khasenov and Turdybekov.[40] They used semiempirical calculations to study the transannular cyclization of 1(10)E,4E-germacranolide costunolide into eudesmanolides and calculated the associated conformers and the energetic barriers. However, they did not approach the problem of the biogenetic origin of the different compounds under study. In contrast, this study will approach the biogenesis of pseudoguaianolides from germacranolides using computational methods as well as experimental data to evaluate the importance of enzymatic participation in the process of cyclization and transposition. The capability of the density functional theory (DFT) hybrid methods: B3LYP,[41] B97−2,[42]B1B95[43] and mPWB95[44] functionals and the MP2[45] method to describe the potential energy surface associated with these compounds (PES) was also evaluated.

It is relatively easy to transform 4,5-epoxygermacranolides to guaianolides using cyclizations catalyzed by Lewis acids.[46] The same is true for the transformation of 4,5-epoxyguaianolide to pseudoguianolides.[47] However, the biomimetic transformations of a germacranolide into the third biogenetic stage are rare. Pseudoguaianolides are formed from the third biogenetic stage and typically contain a nonregular isoprene skeleton with a methyl group at C5. The first successful experiment for the transformation of a germacradiene derivative into a pseudoguaianolide was the transformation of 4α,5*β*-epoxyinunolide (**8**, Scheme 2), isolated from *Stevia tephrophylla* Blake into inuviscolide (**9**, yield 1.8%), 4α,5α-epoxy-10α,14H-inuviscolide (**10**, yield 1%) and 8-epiconfertine (**11**), a pseudoguaianolide (yield 4.1%) using a bentonitic earth.[48] The stereochemistry of the cyclization products is expected if it is assumed that the most stable conformation of the precursor **8** is similar to the conformation of laurenobiolide,[49] in which both methyl groups are above the plane of the cyclodecadiene and the double bond and the epoxide have a crossed orientation, which in Samek's nomenclatures is described as $^{15}D_5,_1D^{14}$ (**8**).[50]

SCHEME 2. Proposed Mechanism for the Transformation of 4α,5*β*-Epoxyinunolide (8) into Inuviscolide (9), 4α,5α-Epoxy-10α,14H-inuviscolide (10) and 8-Epiconfertine (11) through Cations 12 and 13[48]

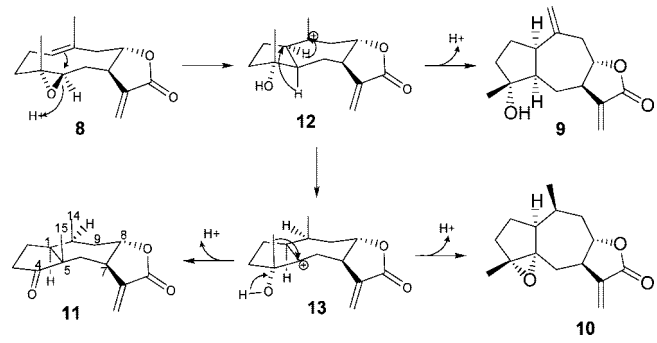

The proposed mechanism is presented in Scheme 2 and is supported in the structure of the isolated byproducts.[48] Within this mechanism, it is proposed that in the first step there is a cyclization of the $^{15}D_5,_1D^{14}$ conformer which produces a *cis*-fused carbocation **12** that yields compound **9** if the methyl group takes part in the elimination reaction. This is the main product when the Lewis or Bröwnsted acids are used.

Carbocation **12** after two consecutive hydride shifts (Scheme 2) produces carbocation **13**, which through an intramolecular nucleophilic attack generates epoxide **10**. Finally carbocation **13** suffers a transposition driven by the formation of the carbonyl group that produces the methyl group migration. Due to the fact that Ortega and Maldonado[48] did not have any more proof of the existence of any other carbocation that takes part in the process, they did not mention other cationic intermediates that would be likely to take part in the process. Then, the issues are which carbocations really exist as intermediates and what is the nature of the transition states (TSs) involved in the process in terms of structure and energy. The other issue that needs to be answered is if this reaction needs enzymatic catalysis or if it is only a "cascade" pathway in which the main role of the enzyme is to start the process activating the electrophilic reaction and stabilizing cationic intermediates to enable the required transpositions. In this case, it is interesting to analyze the role of bentonitic earth because it has two major effects. The first effect is selectivity. Although it lacks the complementary structure, similar to the pattern characteristic of proteins, the bentonitic earth is able to select the starting conformer of the germacradiene. The second one is the capability to stabilize the intermediate cations that might increase their average lifetime. This is why the system may undergo transposition reactions

(27) Gao, D.; Pan, Y.-K.; Byun, K.; Gao, J. *J. Am. Chem. Soc.* **1998**, *120*, 4045–4046.
(28) Rajamani, R.; Gao, J. *J. Am. Chem. Soc.* **2003**, *125*, 12768–12781.
(29) Zhao, Y.; Truhlar, D. G. *J. Org. Chem.* **2007**, *72*, 295–298.
(30) Ho, G. A.; Nouri, D. H.; Tantillo, D. J. *J. Org. Chem.* **2005**, *70*, 5139–5143.
(31) Gutta, P.; Tantillo, D. J. *J. Am. Chem. Soc.* **2006**, *128*, 6172–6179.
(32) Gutta, P.; Tantillo, D. J. *Org. Lett.* **2007**, *9*, 1069–1071.
(33) Hong, Y. J.; Tantillo, D. J. *Org. Lett.* **2006**, *8*, 4601–4604.
(34) Kürti, L.; Chein, R.-J.; Corey, E. J. *J. Am. Chem. Soc.* **2008**, *130*, 9031–9036.
(35) Jenson, C.; Jorgensen, W. *J. Am. Chem. Soc.* **1997**, *119*, 10846–10854.
(36) Hess, B. A., Jr. *J. Am. Chem. Soc.* **2002**, *124*, 10286–10287.
(37) Hess, B. A., Jr. *Org. Lett.* **2003**, *5*, 165–167.
(38) Hess, B. A., Jr. *Eur. J. Org. Chem.* **2004**, *223*, 9–2242.
(39) Hess, B. A., Jr.; Smentek, L. *Org. Lett.* **2004**, *6*, 1717–1720.
(40) Khasenov, B. B.; Turdybekov, K. M. *Chem. Nat. Prod.* **2001**, *37*, 451–454.
(41) Becke, A. D. *J. Chem. Phys.* **1993**, *98*, 5648–5652.
(42) Wilson, P. J.; Bradley, T. J.; Tozer, D. J. *J. Chem. Phys.* **2001**, *115*, 9233–9242.
(43) Becke, A. D. *J. Chem. Phys.* **1996**, *104*, 1040–1046.
(44) (a) Zhao, Y.; Truhlar, D. G. *J. Phys. Chem. A* **2004**, *108*, 6908–6918. See also: (b) Zhao, Y.; Truhlar, D. G. *Acc. Chem. Res.* **2008**, *41*, 157–167.
(45) (a) Head-Gordon, M.; Pople, J. A.; Frisch, M. J. *Chem. Phys. Lett.* **1988**, *153*, 503–506. (b) Frisch, M. J.; Head-Gordon, M.; Pople, J. A. *Chem. Phys. Lett.* **1990**, *166*, 275–280. (c) Frisch, M. J.; Head-Gordon, M.; Pople, J. A. *Chem. Phys. Lett.* **1990**, *166*, 281–289. (d) Head-Gordon, M.; Head-Gordon, T. *Chem. Phys. Lett.* **1994**, *220*, 122–128. (e) Saebo, S.; Almlof, J. *Chem. Phys. Lett.* **1989**, *154*, 83–89.
(46) For the transformation of epoxygermacranolides in to guaianolides see: (a) White, E. H.; Winter, R. E. K. *Tetrahedron* **1963**, *19*, 137–141. (b) Govindachari, T. R.; Josi, B. S.; Kamat, V. N. *Tetrahedron* **1965**, *21*, 1509–1519. (c) Gaissman, T. A.; Ellestad, G. A. *Phytochemistry* **1971**, *10*, 2475–2485. (d) Griffin, T. S.; Geissman, T. A.; Winters, T. W. *Phytochemistry* **1971**, *10*, 2487–2495. (e) Irwin, M. A.; Lee, K. H.; Simpson, R. F.; Geissman, T. A. *Phytochemistry* **1969**, *8*, 2009–2012.
(47) For the transformation of 4,5-epoxyguaianolide in to pseudoguianolides see: Fischer, N. H.; Wiley, R. A.; Perry, D. L. *Rev. Latinoam. Quim.* **1976**, *7*, 87–93.
(48) Ortega, A.; Maldonado, E. *Heterocycles* **1989**, *29*, 635–638.
(49) Takeda, K. *Tetrahedron* **1974**, *30*, 1525–1534.
(50) Samek, Z.; Harmatha, J. *Collect. Czech. Chem. Commun.* **1978**, *43*, 2779–2799.

before undergoing eliminations and, as a consequence, the formation of more advanced biogenetic derivatives.

Methods

All the quantum chemical calculations were performed with Gaussian 03.[51] Geometries were optimized without geometry constraints using the DFT hybrid method with B3LYP, B97−2, B1B95 and mPWB95 functionals and the MP2 method. The double split valence polarized and diffuse 6−31+G(d,p) basis set was used for geometry optimization and frequency calculations. All energies were reported with zero-point energy corrections and are not scaled for comparative purpose. The 6−31+G(d,p) basis functions were used due to the fact that addition of diffuse functions to double split valence basis has shown to be more important than increasing to a triplet split valence basis when calculating reaction energies and activation energies with DFT.[52]

The B3LYP functional has been used to calculate structures for TSs of carbocations, reaction energies and activation energies of hydride shifts and cyclization energies.[30,31,33,53−56] However it is well-known that the popular B3LYP method usually underestimates barrier heights.[57,58] Moreover, other studies have shown that the B3LYP method fails on the prediction of the structure of a protonated epoxide[29,59] and of triterpene cyclization energies.[60] On the other hand, newer functionals have been developed such as mPWB95 and B1B95 that include the kinetic energy density of electrons as correction factor. Recent studies in small systems have shown that the second generation B97−2 functional and third generation B1B95 and mPWB95 functionals produce more reliable results than the B3LYP functional.[61,62]

We compared DFT TS energies and structure with the MP2 method to find if new functionals in such large systems correct activation energies in the right direction because it is well know that the MP2 method tends to be inaccurate in the energy evaluation for such systems in the opposite direction from DFT.[63] Finally, NBO analysis was carried out with version 3.1 included in Gaussian 03.[64]

Results and Discussion

First, we determined whether the mechanism proposed by Ortega and Maldonado[48] (Scheme 2) is energetically feasible. The energy of the fully geometry-optimized intermediates and TSs for the pathway from protonated epoxyinunolide cation to protonated 8-epiconfertin cation are shown in Figure 1 and the relative energy is in Table 1. As a reference point we used cation **14**. In conformer $^{15}D_5$, $_1D^{14}$, with chair−chair arrangement (see **8**, Scheme 2), the transanular distance between C1 and C5 is merely 2.93 Å at mPWB95/6−31+G(d,p). A reasonable first step in this mechanism after protonation of the epoxide at the oxygen atom could be a C5−O bond break; this would leave a classical secondary carbocation at C5 as intermediate. However, all attempts to find the carbocation at C5 converge in **14** or in an intermediate in which the charge deficiency is located at C10 (**16**). This indicates that the global transformation occurs in only one step. Therefore, we searched throughout the Potential Energy Surface (PES) for the TS that allows the interchange between these two minima, shown as **15** in Figure 1.

In TS **15** we show how distance C1−C5 is shortened with the corresponding increase of the C5−O distance, so the distance of the transannular interaction goes from 2.93 Å in **14** to 2.64 in **15** and forms a C−C bond of 1.64 Å in **16**. It can be stated that this elementary reaction occurs through the TS **15** with high delocalization. Even when many changes occur in the molecular structure of the compounds involved, the activation energy is low (Table 2). Results at MP2 level suggest a higher relative energy, while functional B3LYP the lowest. The second and third generation functionals predict energies that fall between these two methods.

Intermediate **16** lacks the proper conformational arrangement to allow the required [1,2] hydrogen shift, the next step in the transformation. The plane that forms C1−C10−C14 is parallel to the C−H that must be transferred, and this chemical process requires that the transferring bond be perpendicular to the plane of the referred atoms. Recently, it was described that the undertaking of conformational analysis requires considering the conformational process as a sequence of elementary conformational steps.[65] Hence, it is necessary to establish the way in which the stationary states of minimum energy are interconnected through the TS. This is feasible for cation **16** which is transformed into conformer **18** through TS **17** (Figure 2). In this TS, the angle C14−C10−C1−C5 reaches a value of 145° (level mPWB95). The stabilization of cation **17** is due to hyperconjugation by the participation of two σ_{C-C} bonds (C1−C5 and C8−C9) and a σ_{C-H} bond of the methyl group.[66] At mPW95/6−31+G(d,p) level the distance C1−C5 is 1.64 Å, the C8−C9 of 1.55 Å and C15−H is 1.10 Å, larger than C15−H distance of the other hydrogen atoms of the methyl group. The NBO analysis of these $\sigma_{C-H} \rightarrow \pi$ interactions establishes values of 25.4, 13.4 and 15.8 kcal/mol respectively for each interaction at mPWB95/6−31+G(d.p).

In cation **18** (Figure 1), the product of the conformational change, there are three hydrogen atoms that hyperconjugate to produce stabilization. The C1−H distance is 1.13 Å, the C9−H is 1.10 Å and C15−H is 1.10 Å and coincides with the energy stabilization values determined by NBO analysis at mPW95/6−31+G(d,p) level which are 54.8, 14.8 and 18.0 kcal/mol, respectively.

The elimination reaction would take place in **18**, generating any of the 3 possible olefins. In the case under study, compound **9** (Scheme 2) is originated through the loss of one of the

(51) Frisch, M. J.; et al. *Gaussian 03*, revision D.01; Gaussian, Inc.: Wallingford, CT, 2004.
(52) Lynch, B. J.; Zhao, Y.; Truhlar, D. G. *J. Phys. Chem. A* **2003**, *107*, 1384–1388.
(53) Vrček, V. *Int. J. Quantum Chem.* **2007**, *107*, 1772–1781.
(54) Joshi, Y. V.; Bhan, A.; Thomson, K. T. *J. Phys. Chem. B* **2004**, *108*, 971–980.
(55) Vrček, I. V.; Vrček, V.; Siehl, H. *J. Phys. Chem. A* **2002**, *106*, 1604–1611.
(56) Vrček, V.; Vrček, I. V.; Siehl, H. *J. Phys. Chem. A* **2006**, *110*, 1868–1874.
(57) Durant, J. L. *Chem. Phys. Lett.* **1996**, *256*, 595–602.
(58) Lynch, B. J.; Fast, P. L.; Harris, M.; Truhlar, D. G. *J. Phys. Chem. A* **2000**, *104*, 4811–4815.
(59) Carlier, P. R.; Deora, N.; Crwford, T. D. *J. Org. Chem.* **2006**, *71*, 1592–1597.
(60) Matsuda, S. P. T.; Wilson, W. K.; Xiong, Q. *Org. Biomol. Chem.* **2006**, *4*, 530–543.
(61) Zhao, Y.; Pu, J.; Lynch, B. J.; Truhlar, D. G. *Phys. Chem. Chem. Phys.* **2004**, *6*, 673–676.
(62) Zhao, Y.; Truhlar, D. G. *J. Phys. Chem. A* **2005**, *109*, 5656–5667.
(63) Fărcaşiu, D.; Lunkinskas, P.; Pamidighantam, S. V. *J. Phys. Chem. A* **2002**, *106*, 11672–11675.
(64) (a) Carpenter, J. E.; Weinhold, F. *J.Mol. Struct. (Theochem)* **1988**, *169*, 41–62. (b) Foster, J. P.; Weinhold, F. *J. Am. Chem. Soc.* **1980**, *102*, 7211. (c) Carpenter, J. E. PhD thesis, University of Wisconsin, Madison, WI, 1987. (d) Reed, A. E.; Weinhold, F. *J. Chem. Phys.* **1983**, *78*, 4066–4073. (e) Reed, A. E.; Weinhold, F. *J. Chem. Phys.* **1985**, *83*, 1736–1740. (f) Reed, A. E.; Weinstock, R. B.; Weinhold, F. *J. Chem. Phys.* **1985**, *83*, 735–746. (g) Reed, A. E.; Curtiss, L. A.; Weinhold, F. *Chem. Rev.* **1988**, *88*, 899–926.
(65) (a) Fernández-Alonso, M. C.; Asensio, J. L.; Cañada, F. J.; Jiménez-Barbero, J.; Cuevas, G. *Chem. Phys. Chem.* **2003**, *4*, 748–753. (b) Fernández-Alonso, M. C.; Cañada, J.; Jiménez-Barbero, J.; Cuevas, G. *Chem. Phys. Chem.* **2005**, *6*, 671–681.
(66) Laube, T. *Acc. Chem. Res.* **1995**, *28*, 399–405.

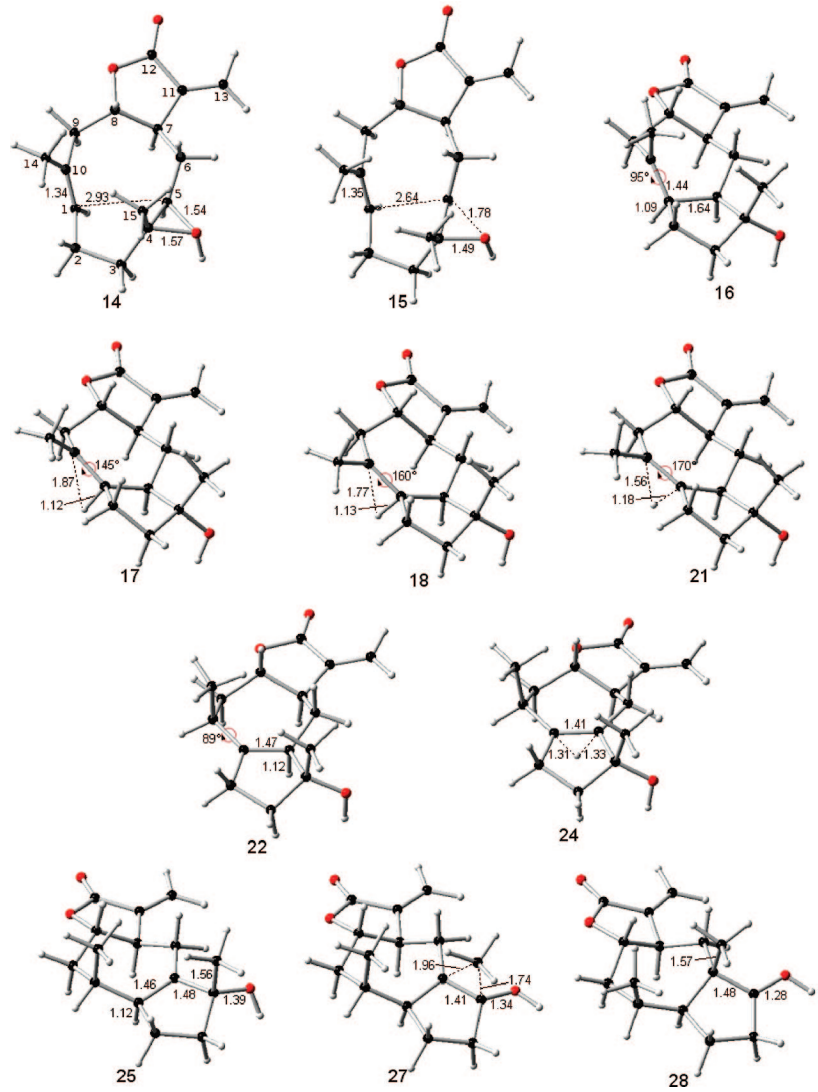

FIGURE 1. Reaction intermediates and TS structures for the conversion of epoxyinunolide cation **14** to 8-epiconfertin cation **28** at mPWB95/6−31+G(d,p) level. Selected distances and C14−C10−C1−C5 dihedral are shown in Å and in degrees, respectively.

TABLE 1. Calculated Relative Energies (in kcal/mol)

	B3LYP		B97–2		B1B95		mPWB95		MP2	
cation	ΔE	ΔE + ZPE	ΔE	ΔE + ZPE	ΔE	ΔE + ZPE	ΔE	ΔE + ZPE	ΔE	ΔE + ZPE
14	0.00	0.00	0.00	0.00	0.00	0.00	0.00	0.00	0.00	0.00
15	0.79	0.52	1.34	0.94	1.71	1.02	1.83	1.00	4.06	1.76
16	–14.62	–14.15	–16.49	–16.11	–16.05	–16.28	–16.26	–16.53	–16.50	–13.74
17	–	–	–	–	–12.63	–13.68	–12.84	–13.89	–15.97	–10.05
18	–	–	–	–	–12.69	–13.85	–12.99	–14.14	–	–
21	–9.64	–11.04	–12.96	–14.22	–12.50	–14.18	–12.82	–14.54	–	–
22	–19.40	–19.66	–22.04	–22.35	–21.39	–21.93	–21.77	–22.32	–25.80	–19.19
24	–14.56	–15.91	–18.27	–19.60	–18.06	–19.79	–18.42	–20.21	–20.83	–18.13
25	–18.80	–19.52	–21.47	–22.09	–21.26	–22.29	–21.66	–22.79	–24.83	–18.60
27	–13.56	–12.99	–16.83	–16.34	–18.63	–18.38	–19.07	–18.92	–16.82	–16.45
28	–27.91	–25.92	–31.03	–29.13	–32.08	–30.29	–32.62	–30.89	–34.50	–29.47

hydrogen atoms of the methyl group, but the described lactones **19** (Chart 2), isolated from *Postia bombycina,*[67] and **20,** isolated from *Helichrysum dasyanthum,*[68] correspond to the other two elimination routes. Lactone **23**, isolated from *Inula thapsoides,*[69] is a good example of the product generated when the cation is trapped by water, but with larger oxidation state at the cyclopentane ring.

(67) Rustaiyan, A.; Zare, K.; Biniyaz, T.; Fazlalizadeh, G. *Phytochemistry* **1989**, *28*, 3127–3129.

(68) Jakupovic, J.; Zdero, C.; Grenz, M.; Tsichritzis, F.; Lehmann, L.; Hashemi-Nejad, M.; Bohlmann, F. *Phytochemistry* **1989**, *28*, 1119–1131.

(69) Topcu, G.; Öksüz, S.; Herz, W.; Díaz, J. G. *Phytochemistry* **1995**, *40*, 1717–1722.

TABLE 2. Calculated Activation Energies $\Delta E^{\ddagger}$ for the Conversion of 14 to 28 (in kcal/mol)

TS	B3LYP	B97–2	B1B95	mPWB95	MP2
15	0.52	0.94	1.02	1.00	1.76
17[a]	–	–	2.60	2.63	3.69
21[b]	3.11	1.88	2.10	1.98	–
24	3.75	2.75	2.14	2.12	1.06
27	6.53	5.75	3.92	3.87	2.15

[a] Energy difference between **17** and **16**. [b] Energy difference between **17** and **21**.

Through the conformational change, it is possible to modify the substitution pattern of the bond type that participates in the stabilization of the cation by hyperconjugation.[70] Two C−C bonds were changed to two C−H bonds that according with NBO analysis are more efficient for the stabilization of the cation. In accordance with the NBO analysis, C10 has an sp^2 hybridization. Nevertheless, the bond angle C1−C9−C10 is 125.9°. This contrasts with the 120.1° measured by the same angle in cation **16**. NBO analysis makes it possible to establish an sp^2 hybridization for the same atom. This is most dramatic when considering C1, since the C10−C1−C5 angle in **16** is 107.2° and in **18** it is 128.4°. The C1 hybridization is of a slightly higher order than sp^2. The energy gained by hyperconjugation is smaller than the energy lost by angular tension; hence, **16** is 2.38 kcal/mol more stable than **18**.

With the adequate conformation, an [1,2]-hydrogen shift is experienced through TS **21** (Figure 1), where the hydrogen atom is found at a distance of 1.18 Å (at a mPWB95/6−31+G(d,p) level) and barely at 1.56 Å of the destination carbon. Concurrently with migration, an adjustment of angle C14−C10−C1-C5 is produced, which goes to 170° in TS **21** and finishes at 89° in product **22**. The asynchrony of TS **21** is noteworthy. The natural charge of the hydrogen atom which migrates is 0.42 in TS **21**, while in **22**, it is of 0.31 and in **16** it is of 0.32. At C1 the charge is −0.38, −0.25, 0.51 and in C10 is 0.48, 0.32 and −0.38 for compounds **16**, **21** and **22** respectively, at mPWB95/6−31+G(d,p) level of theory. From the above, it can be concluded that in the TS the positive charge is delocalized mainly between the two carbons; even if it is also delocalized toward the hydrogen atom. Apparently, the hydrogen atom instead of migrating as a hydride as it is usually believed, migrates as a proton. However, the charge found using the computational methods may not be a definitive criterion. The stability of cation **22** comes from the hyperconjugation of one σ_{C-C} bond and two σ_{C-H} bonds.

In this global process, we found that the number of elementary steps strongly depends on the calculation method (Figure 2). Curiously, the reaction trajectories that describe the two levels are parallel and can be partially superposed (see the IRC projection on the lower part of the scheme). However, while intermediates **17** and **18** are stable stationary states at the mPW95/6−31+G(d,p) level, (Figure 2a) at the B3LYP/6−31+G(d,p) level they are only another point on the reaction trajectory (Figure 2b). Additionally, the position of TS **21** is different at the two levels of theory.

At the mPWB95 and B1B95 levels we found two TSs. The first one corresponds to the conformation rearrangement (**17**) and the other corresponds to the hydrogen shift (**21**). But at B3LYP and B97−2 we did not find **17** and at the MP2 level, **21** does not exist. This is because the potential energy surface

(70) Juaristi, E.; Cuevas, G. *Acc. Chem. Res.* **2007**, *40*, 961–970.

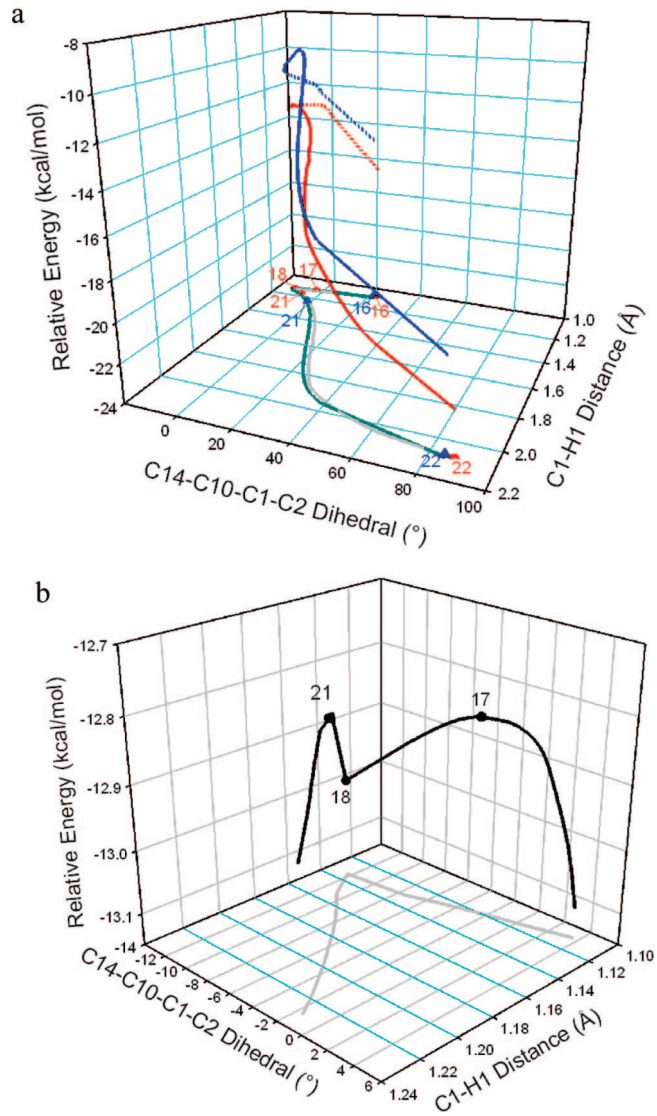

FIGURE 2. (a) Intrinsic reaction coordinate (IRC) for the transformation of cation **16** to cation **22** at mPWB95/6−31+G(d,p) (red) and B3LYP/6−31+G(d,p) (blue) levels of theory and projection of the IRC at mPWB95/6−31+G(d,p) in dark gray and projection of the IRC at B3LYP/6−31+G(d,p) in gray. All energies are relative to **14**. (b) Enlargement of the 17−18−21 intermediates section at mPW95/6−31+G(d,p) level.

is too flat in the TS region (Figure 2 and Table 1), and the shape of the potential surface in this region depends extremely on the level of calculation. Even at mPWB95 and B1B95 levels, the zero-point corrected energy of intermediate **18** is higher than the zero-point corrected energy of **21** (Table 1). Although at some theory levels, there is only a single-step.

At this point, the conditions that favor the occurrence of the second migration are present in intermediate **22**, the hydrogen atom that will take part in that migration has the required geometry for this purpose as it maintains a *syn* relation respect to the hydrogen atom that migrates from C1 to C10. In this case, **22** and **25** are almost isoenergetic and the barrier height is smaller than that of other similar cases.[31,55,56] This migration is highly symmetric, since in the TS the C1−H distance is 1.31 Å and the C5−H distance is 1.33 Å. This stems from the fact that the two cations connected by TS **24** have a similar substitution pattern at the level of first neighbors. The existence of cation **25** is certainly proven by the isolation of epoxide **10**

SCHEME 3. Lactones Isolated from the Aerial Parts of *Apalochlamys spectabilis* (Labill.) J.H. Willis

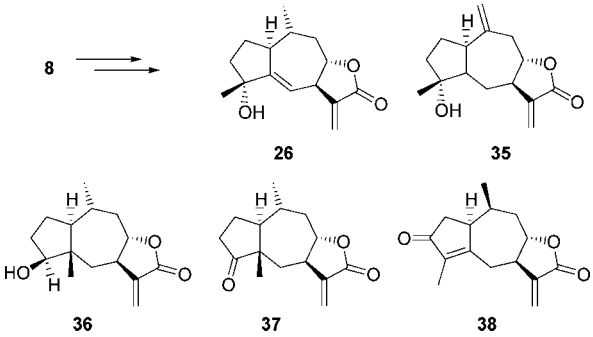

(Scheme 2), but the elimination product has also been found in **26** (epimer of carbocation **25**, Scheme 3).[71]

Finally, 8-epiconfertin cation (**28**) is accessed through [1,2]-methyl shift from **25**. The methyl group is found in the TS at 1.74 Å from the origin and at 1.96 Å from the destination atom. This makes it more similar to **25** than to the product **28**. Therefore, in accordance with Hammond's postulate, an exothermic reaction is expected when the product is generated. This is evident by the observations where the process concludes with the hydrogen atom joined to the carbonyl group. In fact, this bond evolved from 1.39 Å in the intermediate, to 1.34 Å in the TS and finally to 1.28 Å in the product. It is worth noting that the depletion of charge in cation **28** is concentrated between C4 and O, since the C4 natural charge goes from 0.17 in **25** to 0.74 in **28** and the charge of the oxygen atom goes from −0.74 in **25** to −0.59 in **28**.

In general, this last step has the largest activation energy in 8-epiconfertin formation. This may explain why it is possible to isolate the products where epoxide **10** is formed (by trapping the cation).

This mechanism is in complete agreement with experimental results[48] due to the fact that there is an intermediate for each byproduct. Then one question that remains unanswered is if this transformation needs enzymatic catalysis. It might seem that it is not necessary because the whole process occurs like a "cascade" pathway (Figure 3). All barrier heights are very small, less than 4 kcal/mol, and the activation energy for the first step is even smaller. In fact, ambient thermal energy would be enough to reach this barrier. So once the molecule is protonated, the whole process occurs without help of any enzyme. Nevertheless, it has been suggested that the enzyme has more than a catalytic function, a fundamental role in the conformational adjustment which generates the selectivity of the subsequent cyclizations. Is this function relevant?

Two fused *trans*-pseudoguaianolide groups are well-known. The first one is the ambrosanolides, belonging to the subtribe Abrosinae and genus Parthenium. The second group includes the helenanolides, belonging to tribe Heleniae. The structural difference between the two groups resides in the stereochemistry of the methyl group at position C10. The absolute stereochemistry of the stereogenic center supporting the methyl group in the ambrosianolides is *S* while in helanolides is *R* (Chart 3). It is very interesting to underline the fact that the scheme originally proposed by Hendrickson does not explain the stereochemistry of the lactone group denominated as heleanolide. Parker et al.[12] proposed a first hypothesis where they should biogenetically

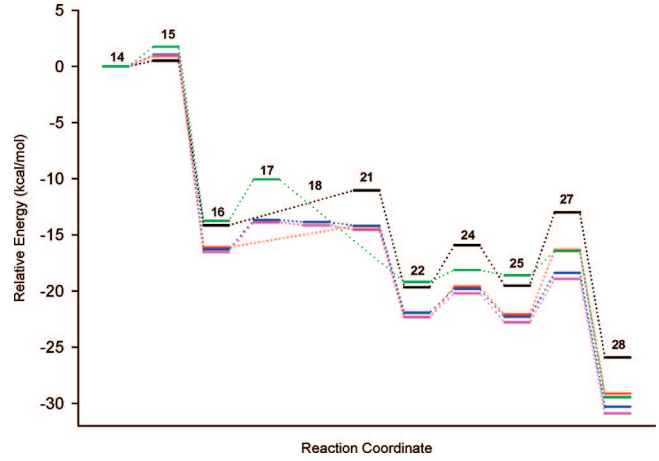

FIGURE 3. Energy diagram for the conversion of epoxyinunolide cation **14** to 8-epiconfertin cation **28.** All energies are relative to **14**. Black lines are results from B3LYP, red from B97−2, blue from B1B95, pink from mPWB95 and green from MP2.

CHART 3

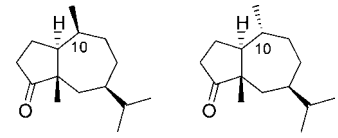

come from a germacradiene with a Z configuration at the C1−C10 double bond (melampolide, **4**, Scheme 1). Fischer[24] proposed a different alternative suggesting that a different conformer of the same germacrediene is responsible for the second series of compounds.

The mechanism described here starts from conformer **14** $^{15}D_5$, $_1D^{14}$ (Figure 4). At a mPWB95/6−31+G(d,p) level, the 4α,5β-epoxyinunolide with $^{15}D_5$,$^1D_{14}$ conformation (**30**) is only 0.89 kcal/mol less stable than **14**. The relative energy for the ring closure process of both conformers is shown in Figure 4, where the conformational equilibrium between **14** and **30** have a activation energy of 12.21 kcal/mol. The analysis of the normal modes of this TS makes it possible to establish that stationary states **14** and **30** are interconnected through TS **29**. In **29**, the substituents at the double bond C1−C10 are practically located in the molecular plane with the hydrogen atom at carbon C1 oriented inside the 10-member ring avoiding the steric crowding associated with the methyl group.

Conformers **14** and **30** are of main interest because their closure defines the stereochemistry of the methyl group at position 10. When the reaction occurs through the more stable conformer **14**, the intermediates presently discussed are produced, leading to carbocation **16.** Nevertheless, when the less stable conformer **30** is analyzed, the ring closure mechanism also occurs in a concerted way through TS **31** (Figure 4) which can be found at 1.18 kcal/mol in relation to the conformer that produces it, and at a 2.07 kcal/mol in relation to conformer **14**. The more stable TS shows the methyl groups confront each other, a sterically unfavored relationship. This is in agreement with published results, making possible to establish that the so-called 1,3-syndiaxial repulsion does not have a main role in the conformation.[72] The conformational properties of this system

(71) Zdero, C.; Bohlmann, F.; King, R. M. *Phytochemistry* **1990**, *29*, 3201–3206.

(72) Cortés-Guzmán, F.; Hernández-Trujillo, J.; Cuevas, G. *J. Phys. Chem. A* **2003**, *107*, 9253–9256.

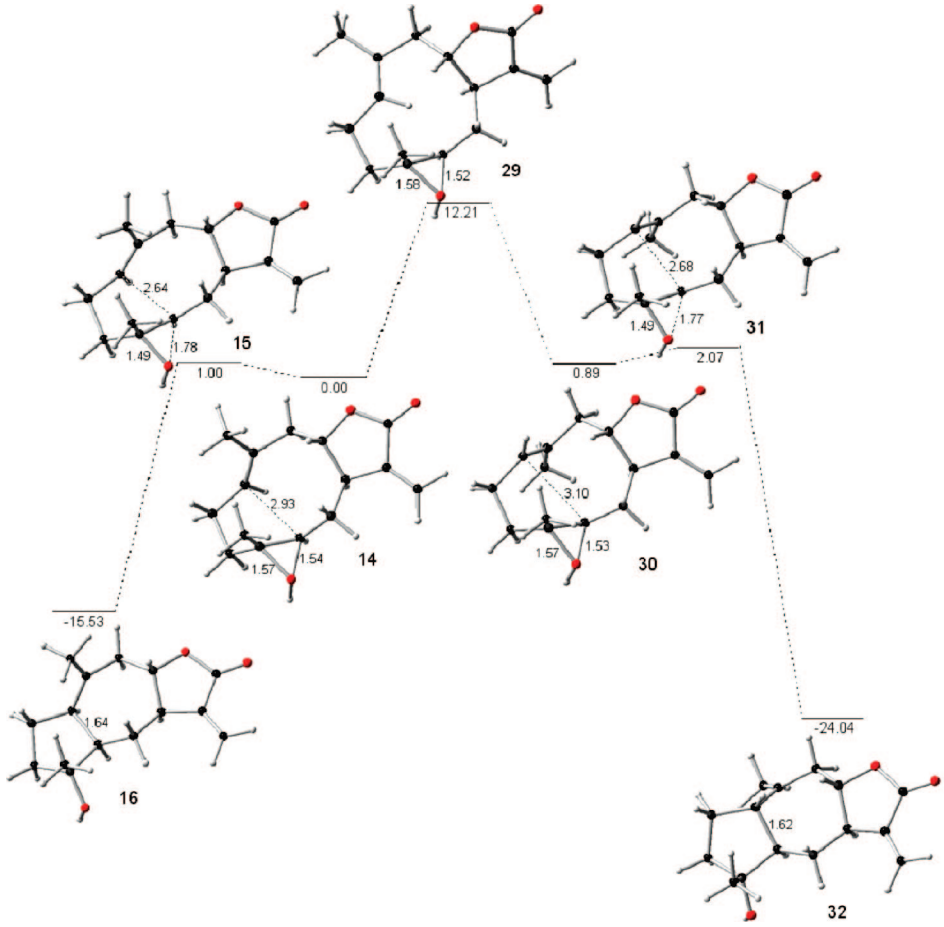

FIGURE 4. Relative energies of conformers **14** and **30**, stationary states associated with the cyclization mechanisms. Relative energy in kcal/mol determined at mPWB95/6−31+G(d,p).

is due to the fact that the 10-member ring (rigid in three points, one of them due to the double bond, the second one due to the epoxide and the third one due to the *trans*-diequatorial lactone) adopts a chair-chair conformation favoring the proximity of the olefin and the epoxide.

Coming back to the annular closure problem, TS **31** generates the thermodynamic product **32** that is 7.51 kcal/mol more stable than the kinetic product **16**. Intermediate **32** generates the epimeric compounds of the whole series. The kinetic product owes part of its instability to the contribution of the methyne groups forming the fusion that are found practically eclipsed. This eclipsing is the origin of the rotational barrier of ethane. In our case, the H−C1−C5−H angle is 9°.

Therefore, ambrosanolides and helenanolides have their origin, in accordance with what is hereby described, in the germacradiene conformer selected (or its corresponding monoepoxide). The application of the Curtin-Hammet principle over the small difference in energy between transition states **15** and **31** (even when the corrections that allow the calculation of enthalpy and the determination of the enthropy are not considered), we could expect that the two C10 epimers can coexist in each species. In general this does not happen because usually only one epimer is found in each natural source. From these results, the relevance of the enzyme that catalyzes the process can be inferred. Interestingly, the compounds obtained by chemical transformation employing bentonitic earth in the paper by Ortega and Maldonado[48] imply the more stable conformer.

Bohlmann et al.[71] also proposed the hypothesis, without clear evidence to support it, that lactones **26** and **35** (Scheme 3) isolated from the aerial parts of *Apalochlamys spectabilis* (Labill.) J.H. Willis, should have a biogenetic origin in compound **8**. This is clear from conformer $^{15}D_{5,1}D^{14}$ (**30**) and by the isolation of intermediates originated by cations derived from of guaianolides. Bohlmann et al.[26] also described the isolation of lactones **36**−**38** from the aerial parts of *Ondetia linearis*. These intermediate products demonstrate that the reaction mechanism for conformer **30** is similar to that described for conformer **14**. The relevant aspect of lactone **36**−**38** is that it is possible, but unusual, to find natural products with both configurations at C10 within the same plant. Therefore, the mechanisms of reaction of both isomers can coexist.

The mechanisms described hereby support the hypothesis of Fischer,[24] who proposed that the transposition occurs through a different conformer. There is an additional proposal suggesting that the transformation of the guaianolide to pseudoguaianolide occurs in only one step.[13] The migration of the methyl group at C4 as well as the migration of the two hydrogen atoms with the elimination of a nucleofuge previously added to cation **16** requires only one TS. This is impossible, based on the results presented in this paper, since several attempts to optimize this TS were fruitless. This would be due to the fact that carbon C10 does not satisfy the stereochemical requirement that allows the migration of the hydrogen atom from position 1. It is necessary to remember that at mPWB95/6−31+G(d,p) level, intermediate **16** must be transformed into conformer **18** through

TS **17**. In this case a concerted mechanism, as those proposed by Herz,[13] requires the fulfillment of all stereochemical requirements and this is not the case, or even worst, **16** is not transformed in **28** in one step. On the other hand Tantillo described that this is not always true and that the connected mechanism requires simultaneous alignment for all relevant orbitals.[73] The reaction trajectories that are described by the mPWB95 and B3LYP levels are somewhat parallel even when in the case of the B3LYP functional a new trajectory could be formed. This new trajectory could be more direct or even shorter between intermediates **16** and **21**. This brings about a new question; why are these trajectories almost parallel? One plausible explanation would be that during the course of the reaction a conformational change happens. This change allows the correct alignment of the orbitals that favors the migration of the hydrogen atom that is under stereoelectronic control.[74] Even when B3LYP is not able to establish stationary states in this case, the trajectory brings about the alignment of the orbitals involved in the migration. If the alignment were not relevant, the reaction trajectory would be completely independent of the conformational change between stationary states **16** and **22**. The assertion of Tantillo is true if the structure of intermediate **16** is taken into account. In **16** the relevant orbitals for the migration of the hydrogen atom are not aligned, however the transference of the hydrogen atom does not occur until the conformational change (a point in the IRC, Figure 2) that allows the proper orientation of the σ_{C-H} orbital and the empty π orbital happens. The proper orientation of the orbitals involved is really required for the hydrogen migration.

In all the stationary states analyzed hereby the disposition of the O−H bond was restricted to the conformer that maintains an antiperiplanar arrangement in relation to C4-Me bond, a product of the approximation of the proton below the epoxide, since it is 0.58 kcal/mol more stable than the cation derived from the approximation of the proton above of the epoxide. Nevertheless, it must be expected that in some steps of the mechanism, the participation of the OH bond is superseded by the participation of the lone pair at the oxygen atom. It was found that when a lone pair at oxygen atom is antiperiplanar to methyl C15 in the stationary states **22**, **24** and **25,** a decrease of energy is produced in a magnitude of 2.54, 1.80 and 0.78 kcal/mol, respectively at the mPWB95/6−31+G(d,p) level of theory. These changes generate an increase of the energetic barrier associated to **22** and **24** from 2.12 to 2.86 kcal/mol, while the energetic barrier of **25** to **27** goes from 3.87 to 4.65 kcal/mol. The stabilization of **22** is given mainly, according to the deletion energies obtained by the NBO analysis, by the interaction of σ_{C5-H} with the empty orbital of the carbocation that goes from 31.61 to 36.16 kcal/mol, when the lone pair at oxygen is antiperiplanar to C15. On the other hand, the stabilization of **25** is not produced for this reason, since the interaction σ_{C4-C15} bond with the empty orbital of the carbocation decreases, going from 18.15 to 16.73 kcal/mol at mPWB95/6−31+G(d,p) level of theory when the referred lone pair is maintained antiperiplanar in relation to C15. Due to the fact that in **25** the hyperconjugation with the empty orbital at the carbocation is weakened, **22** is stabilized more than **25**.

Evaluation of the Computational Methods. To get an idea of how reliable are our results obtained with DFT in such a large system and complex mechanisms, we compared the activation energies and TS geometries calculated with DFT and those calculated with MP2 theory. This comparison was done because it its well-known that in general B3LYP and MP2 give errors in opposite directions for organic molecules when the energy is evaluated.[63] This is because the MP2 method overestimates the delocalized structures while B3LYP overestimates the localized structures just as it has been described by Fărcaşiu et al.[63] So if the other functionals produce results between these two levels of theory we have, in our opinion, a better functional to calculate activation energies and TS geometries for such systems. Although the reaction pathway is similar in shape for all functionals and MP2 (Figure 3), we found significant differences between activation energies at MP2 theory and B3LYP functional (Table 2). Differences in barrier height energies around 70% in relation to the activation energy of the method with highest activation energy were observed. However, the difference is much smaller between MP2 and meta-GGA functionals (mPWB95 and B1B95). The difference between barrier heights is approximately only 45% of the height barrier. Geometries of all intermediates are very similar in all cases. However, there are significant differences between DFT TSs geometries and MP2 geometries. As in the case of energies, the geometry difference is greater with the B3LYP functional. With this functional, the largest differences between bond lengths is 0.2 Å, between bond angles is 9° and between dihedral angles is 22°. With the mPWB95 functional, the largest difference between bond length is 0.16 Å, between bond angles is 3° and between dihedral angles is 12°. The largest differences between internal coordinates are those directly related with the reaction coordinate, as we expected. Compound **15** has the largest differences between B3LYP geometry and MP2 geometry because it is the TS with the largest ring, therefore it has more conformational freedom. Although with B1B95 and mPWB95, the largest difference between geometry is with TS **24**. In general, TS geometries calculated by B1B95 and mPWB95 functionals are between MP2 and B3LYP geometries. Although in the case of hydrogen and methyl shifts, the difference is still large and the geometry is not too different from B3LYP geometry. As we have discussed before, mPWB95 and B1B95 are the only functionals that can find compound **17** which also exists at MP2 potential energy surface. Moreover, these functionals find TS **21** which does not exist at the MP2 potential energy surface but exist at B3LYP. For all these reasons, we thought that mPWB95 and B1B95 are better functionals than B3LYP to calculate activation energies and geometries of TSs of similar systems.

Conclusions

The Hendrickson and Fischer theories to explain the biogenetic origin of guaianolides and pseudoguainolides have full computational support since they characterize all the intermediates and TSs associated with the reaction mechanism. The computational results explain the origin of the intermediates isolated for the first time by Ortega and Maldonado,[48] who in

(73) Tantillo, D. J. *J. Phys. Org. Chem.* **2008**, *21*, 561–570.

(74) (a) Deslongchamps, P. *Stereoelectronic Effects in Organic Chemistry*; Pergamon Press: Oxford, 1983. (b) Szarek, W. A., Horton, D., Eds. *Anomeric Effect. Origin and Consequences*; ACS Symposium Series No. 87; American Chemical Society: Washington, DC, 1979. (c) Kirby, A. J. *The Anomeric Effect and Related Stereoelectronic Effects at Oxygen*; Springer: New York, 1983. (d) Juaristi, E.; Cuevas, G. *Tetrahedron* **1992**, *48*, 5019–5087. (e) Thatcher, G. R. J., Ed. *The Anomeric and Associated Stereoelectronic Effects*; American Chemical Society: Washington, DC, 1993. (f) Graczyk, P. P.; Mikolajczyk, M. *Top. Stereochem.* **1994**, *21*, 159–349. (g) Juaristi, E.; Cuevas, G. *The Anomeric Effect*; CRC Press: Boca Raton, FL, 1995. (h) Chattopadhyaya, J. *Stereoelectronic Effects in Nucleosides and Their Structural Implications*; Uppsala University Press: Uppsala, NY, 1999. (i) Perrin, C. L. *Acc. Chem. Res.* **2002**, *35*, 28–34.

a one pot transformation employing bentonitic earth achieved the advancement of 3 biogenetic stages of these compounds, as is described in the introduction: FPP → germacranolide, germacranolide → guaianolide, guaianolide → pseudoguaianolide. In this instance, the transformation occurs through the more stable conformer which is $^{15}D_5$, $^{1}D_{14}$ According to our results, some of the roles of the enzymes which catalyze these reactions at a biological level would be the selection of the starting conformer and the stabilization of the intermediate cations. This makes it possible for them to undergo the transposition instead of the elimination reactions, as is the case for the origin of compound **9** (Scheme 2). Hence, only the next biogenetic stage is observed experimentally.

The transformation mechanism to produce pseudoguaianolides from cation **12** cannot occur in a concerted manner because the conformational adjustment and the migration of hydrogen atoms occur in elemental steps and an only TS that explains the transformation could not be found. The mechanism is driven since the reaction product is always more stable than its antecessor and because barriers are low. The higher barrier is for the migration of the [1,2]-methyl group with the formation of the carbonyl group, the final step in the biogenesis of pseudoguaianolides.

Finally, there is no doubt that the third generation functional mPWB95 recently developed by Truhlar is a good choice because it is the one that show the best performance of the theoretical methods used here to undertake the problems described hereby. It improves the description of the energetic barriers when compared to the B3LYP functional and makes it possible to undertake the study of very planar segments of the potential energy surface where this functional tends to fail.

Acknowledgment. J.E.B.L. acknowledges Conacyt for financial support. We also thank the referees, Prof. Alfredo Ortega and Prof. Leovigildo Quijano, for useful comments. This work was supported by Consejo Nacional de Ciencia y Tecnología (CONACYT) for financial support via grants 49921-Q, and DGAPA grant IN-209606. We are also grateful to DGSCA, UNAM for supercomputer time. We are grateful to Dra. Rebeca López-García and Raquel Feregrino for the revision of the English version of this manuscript.

Supporting Information Available: Energy, Zero Point Energy, and fully optimized geometries of all compounds here described and full ref 51. This material is available free of charge via the Internet at http://pubs.acs.org.

JO802445N